Aerodynamic Characteristics of Airfoils with Blunt Trailing Edge

A. Gómez

M.Sc. Dept. of Mechanical Eng. Universidad de los Andes.
Now Ph.D. student at the University of Hannover, Germany.
gomez@tfd.uni-hannover.de

Álvaro Pinilla

Ph.D, M.Sc. Professor of the Mechanical Engineering
Dept. Universidad de los Andes. Bogotá D.C., Colombia.
apinilla@uniandes.edu.co

RESUMEN El siguiente trabajo estudia de manera computacional el comportamiento de las características aerodinámicas de perfiles NACA (National Advisory Committee for Aeronautics, hoy conocido como NASA), con modificaciones en el borde de salida. Las modificaciones consisten en remover secciones del borde de fuga del perfil. La investigación realizada estudia 39 perfiles diferentes de la familia NACA de 4 dígitos, con modelos teóricos sencillos para explicar los fenómenos. Los resultados muestran los cambios en las características de sustentación y arrastre del perfil, y cambios en cuanto a la entrada en pérdida del mismo.

ABSTRACT This paper is a computational study of the behaviour of aerodynamic characteristics of NACA (National Advisory Committee for Aeronautics, today known as NASA) profiles with tailored trailing edges. 39 different profiles 4-digit NACA family were studied during the research. A computational research was made, using simple theoretical models to explain and to understand the results. The results describe the changes in lift and drag characteristics and changes in stall angle of attack.

INTRODUCTION

Traditionally, airfoil geometries are such that they have a rounded leading edge and a sharp trailing edge. It would be useful in some cases, to use airfoil geometries which are thicker, in order to attain better structural performance. The following paper studies the effects on the aerodynamic performance caused by modifications made to the trailing edge of subsonic profiles, intended for use in wind turbines. The type of modifications proposed can be summarized as cutting off the trailing edge perpendicular to the chord line of the profile at different positions along the chord. In the early 1950's, NACA (National Advisory Committee for Aeronautics) undertook a series of investigations to conclude about the benefits of tailoring the trailing edge of supersonic and transonic profiles [1-4]. The conclusions of these studies can be summarized as an increase in the maximum lift coefficient, and increase in profile drag, and an increase in the lift coefficient slope. The following paper studies similar results for subsonic profiles. The results found include an increase of maximum lift coefficient, a delay in stall and an increase in profile drag. This paper describes how the C_l, C_d, and C_l/C_d curves change as modifications to the trailing edge are made.

Delay in stall of the airfoil could be advantageous for applications such as acrobatic flight, where high angles of attack are needed before the profile stalls. For wind turbines, the fact that higher angles of attack can be reached before entering stalled conditions means that some unsteady effects can be avoided. Namely, when wind gusts or sudden change of wind direction occur, some sections of the wind turbine can stall. This happens mainly in the inboard region of

the blade, where the relative wind speed is lower (and thus more sensitive to variations in angle of attack). These effects can last some time before the boundary layer reattaches (leading edge reattachment) and induce unsteady loads on the rotor blades, which in turn reduce the blades life.

The use of blunt trailing edge profiles for wind turbines at the root of the blades would increase the blade's structural strength. Although the increase of profile drag is responsible for a reduced overall efficiency of the rotor, the disadvantages of a decreased efficiency are overcame, due to the fact that the inboard section of the blades do not account for the mayor part of the power generated. The mayor part of the power generated comes from the blade sections at radial stations between 60-90% of the blade's radius.

In order to understand the aerodynamic characteristics of profiles, a thorough knowledge of the effects that the geometry has on the overall aerodynamic performance is required. It is useful to study theoretically the lift and drag characteristics. For this purpose, Joukowski profiles are studied, along with the theoretical solution of inviscid potential flow around them. Additionally, simple mathematical models are proposed in order to understand, at least in a qualitative manner, the general aspects of the profile's drag and lift after modifications have been made to the trailing edge.

For the purpose of understanding the effects of tailoring the trailing edge, 3549 computer simulations were undertaken for 39 different profiles, cutting off the trailing edge at 7 different chord positions, varying the angle of attack between 0° and 14.6°.

AIRFOIL GEOMETRY

In order to make a computational equivalent of the geometry of the profiles, the original paper presented by NACA in 1932 was used [5]. This paper describes the method used to approximate the profile curves using polynomials.

The studied profiles are as those shown in Fig. 1, which illustrate the type of modifications proposed. The different families of airfoils that were studied correspond to the NACA profiles listed in Table 1. Each of these is composed of different modified airfoils with cut-offs at the trailing edge, ranging from 0% to 30% of the chord, in increments of 5%.

2206	2212	2215	2221
2406	2412	2415	2421
2606	2612	2615	2621
4206	4212	4215	4221
4406	4412	4415	4421
	4612	4615	4621
6206	6212	6215	6221
6306	6312	6315	6321
6406	6412	6415	6421
6606	6612	6615	6621

Table 1. NACA 4-digit series profiles studied.

The profiles were chosen such that a wide range of relative profile thicknesses could be studied, along with different camber geometries.

COMPUTATIONAL SIMULATION

For the CFD simulation, ANSYS CFX was used along with ANSYS CFX-Mesh. A computational control volume around the airfoil is constructed with dimensions 15m × 7m. The grid was constructed using an unstructured mesh and the profile's surface was made up of 2-D extruded elements of 0.01m in length. Additionally, 14 elements within a 5mm region perpendicular to the profile's surface were used to account for boundary layer effects. The inlet and outlet conditions of the control volume consisted respectively of a constant velocity field and an averaged pressure output of 0 Pa (relative to atmospheric pressure). The simulation accounts only for 2-D incompressible flow effects. Table 2 summarizes the parameters used in the simulations.

For each of the simulations that were run, an independent geometry file, mesh, and boundary conditions definition file were needed. The complete study of one family of airfoils requires 91 different simulations.

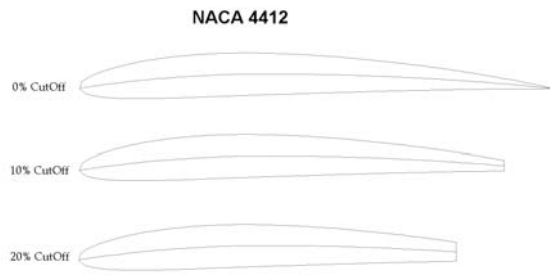| Parameter	Value
Profile Chord	1 m
Inlet velocity	50 m/s
Fluid	Air
Temperature	300 K
Reynolds Number	3.2x106
Mach Number	0.144
Heat Transfer Model	Isothermal
Turbulence Model	k-ε
Profile	Wall (No Slip)
Control Volume Outlet	Average Static Pressure

Table 2. Simulation parameters.

NACA 4412

Figure 1. Modified airfoils at Λ = 0,0.1 and 0.2

Drag forces are caused mainly by two factors. The first one is pressure induced drag, and the second one is viscosity induced drag [6]. Pressure induced drag deals with pressure differences throughout the profile's length, with the pressure at the leading edge being greater than at the trailing edge. Viscosity induced drag deals with boundary layer effects due to the shear forces acting on the fluid. Boundary layer thickness is assumed to be:

$$\frac{\delta}{c} \approx 0.14 \, \mathrm{Re}^{-1/7} \quad .$$

COMPUTATIONAL RESULTS

The CFD simulations are used to produce curves of lift and drag coefficients versus angle of attack of the airfoil. Additionally, the curves of Cl/Cd are also plotted.

Figures 2 to 4 depict an example of the data obtained with the CFD analysis for the NACA 4415 profile, with modifications ranging from 0% cut-off (original airfoil) to 30% cut-off.

The most important characteristics of this family of curves may be summarized as follows:

▪ As the cut-off length increases, the drag coefficient of the airfoil increases (see Fig. 2).

▪ As the cut-off length increases, the lift coefficient decreases (see Fig. 3).

▪ For greater cut-off lengths, the angle corresponding to the maximum C_l/C_d relation ($a_{Cl/Cdmax}$) increases (see Fig. 4).

▪ For greater cut-off lengths, the profile's stall angle is larger (see Fig. 3).

This last characteristic is presumably a consequence that a blunt trailing edge poses a slightly greater resistance to trailing edge separation, due to vortex convection in the stagnation region. This leads to a delay in vortex formation at the trailing edge. There is no computational evidence of the presumption.
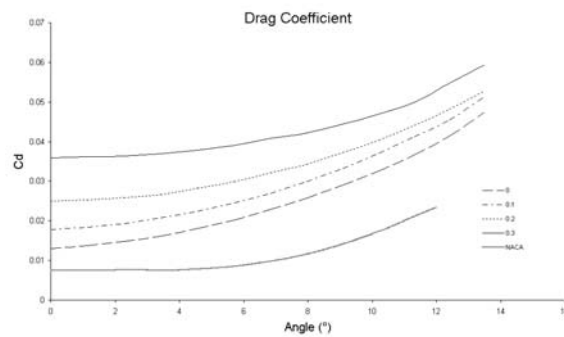

Figure 2. 2-D Drag Coefficient for NACA 4415 [7] for Λ = 0, 0.1, 0.2 and 0.3
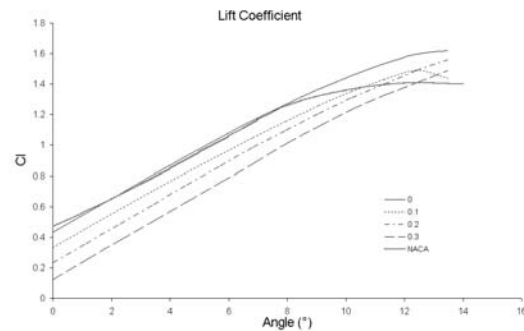

Figure 3. 2-D Lift Coefficient for NACA 4415 [7] for Λ = 0, 0.1, 0.2 and 0.3
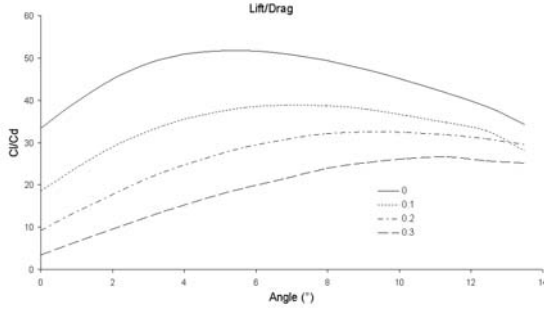
Figure 4. 2-D Lift/Drag ratio for NACA 4415 [7] for Λ = 0, 0.1, 0.2 and 0.3

In wind turbine applications, the blade's geometry is such that angle of attack of the profile coincides with $\alpha_{Cl/Cdmax}$ for nominal power generation. For this reason, the characterization of this curve is very relevant.

For each of the profiles, a Gaussian curve of the form

$$C_L/C_D = a_1 \exp\left(-\left((\theta - b_1)/c_1\right)^2\right) \qquad \text{is}$$

fitted to each of the C_l/C_d graphs (see Fig. 5). The parameters a_1, b_1 and c_1 are to be determined by means of minimum squares methods. For each of the different cut off lengths these parameters are found to be different. A relationship between these parameters and the percentage of cut off at the trailing edge is also found.

A Gaussian fit of this type is useful, because parameters a_1 and b_1 explicitly represent two very important aerodynamic characteristics, namely the

$$\left(C_l/C_d\right)_{max} \text{ and } \alpha_{Cl/Cdmax}$$

respectively. This parameterization allows a_1 and b_1 to be studied as functions of Λ (cut-off length), thus giving a description of the profile's response to trailing edge modifications. Using this parameterization, a correlation between the profile's response to these modifications and its geometrical parameters can be established.

If Λ denotes the cut-off length as a number between 0 and 0.3, then the different parameters can be expressed as a function of Λ for each of the families of airfoils. An example of such parameterizations is shown in Figures 6 and 7. It is interesting to note that the behaviour of parameters a_1, b_1 and c_1 is linear with Λ. These figures depict an example for the profile NACA4415. It is clear from Fig. 6, that when Λ increases, parameter a_1 decreases linearly, that is,

$$\left(C_l/C_d\right)_{max}$$

decreases in proportion to the amount of trailing edge removed. The slope of this line represents a response variable, which is unique to the profile, and describes the sensibility of the profile to the modifications. Steeper slopes (more negative) are a sign of rapid degradation of aerodynamic characteristics as a consequence of trailing edge modifications. In regard to parameter b_1, it can be seen that it increases linearly as Λ increases. The slope of this curve is again a response variable, indicating the degree of sensibility of the profile to the modifications. Larger slopes indicate a more rapid displacement of the

$$C_l/C_d$$

curves to the right (that is a more rapid increase in $\alpha_{Cl/Cdmax}$). Figure 7 shows the variation of parameter c_1, which is in direct relation with the drag coefficient of the profile. From the Gaussian fit it is clear that smaller values of c_1 represent a narrower curve. This is a consequence of a rapid increase in drag coefficient at high angles of attack (thus reducing the C_l/C_d ratio).

Following this parameterization, the 39 studied profiles can be grouped according to a_1, b_1 and c_1 as functions of Λ. For each of the parameters a_1 and b_1 there are two governing variables, namely y-intercept (value of a_1 or b_1 for $\Lambda=0$) and slope

$$\left(\frac{\partial a_1}{\partial \Lambda} or \frac{\partial b_1}{\partial \Lambda}\right).$$

The y-intercept represents a parameter of the profile itself ($\Lambda=0$ means no modification to the trailing edge), while the slope represents a parameter of the response to tailoring the trailing edge. The y-intercept of parameter a_1 represents the maximum C_l/C_d relationship for untailored profiles, and the y-intercept of b_1 represents the angle at which it occurs.

The results of these parameterizations can be seen in Appendix A and B. The graphs on the appendices A and B collect the studied profiles according to their relative thickness and camber. These figures show how depending on these two geometrical features (thickness and camber) the profile's aerodynamic characteristics vary more or less when modifications are made at the trailing edge.

The plots presented in the appendices are guidelines to predict a profile response to trailing edge modifications, correlated with geometrical parameters as thickness and camber. It is seen in Appendix A that thicker profiles are more sensitive to alterations at the trailing edge. This is can be read from the plot as a lower value of ξ (slope of a_1). For applications in which high C_l/C_d are desired, relatively thin profiles should be used. Larger camber also has as consequence lower values of ξ (steeper -more negative- slopes). Appendix B shows the correlation between parameter b_1 and the profile's thickness and camber. It can be seen that profiles with greater thickness and camber achieve greater displacements of $\alpha_{Cl/Cdmax}$. This can be

read as greater values of η, which is the slope of the curve b_1 vs. Λ.

Thus, a compromise must be made between loss in aerodynamic performance and an increase in $\alpha_{Cl/Cdmax}$. For wind turbines at the inboard section, an increase of $\alpha_{Cl/Cdmax}$ is readily translated into lower pitch angles, which in turn results in a more linear distribution of the blade's pitch positioning, and thus a cheaper manufacture. Having these profiles in the inboard region increases the structural stability of the blade because of higher area moments of inertia, and also reduced stress at the root of the blade. The penalty is a lower aerodynamic performance, but as said in the introduction, the inboard section of the blade is not responsible for the mayor percentage of power generation.
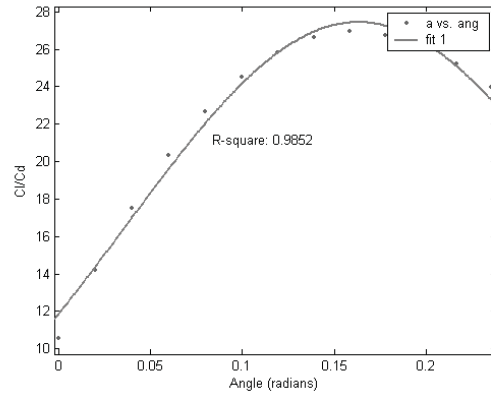

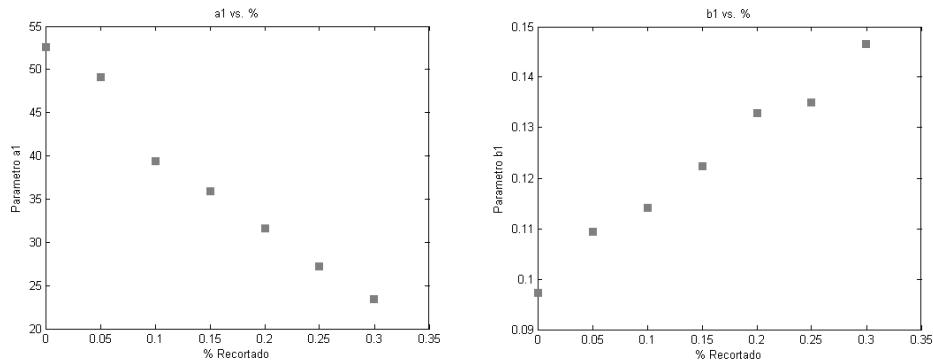Figure 5. Gaussian fit for Cl/Cd for the NACA 6421 with a 20% cut-off. (Drawn with MatLab ©)

Figure 6. Parameters a_1 and b_1 for different Λ's - Airfoil NACA 4415. (Drawn with MatLab ©)

EFFECTS OF LIFT AND DRAG OVER C_L/C_D

In the process of designing rotor blades for applications such as wind turbines, compressors, fans, etc., having a good understanding of the C_l/C_d curves can prove more useful than the C_l and C_d curves alone [8,9]. This is due to the fact that the rotor blades are designed such that at every radial position the profile makes an angle $\alpha_{Cl/Cdmax}$ with respect to the relative wind speed (assuming nominal power extraction and a constant wind field). For this reason, it is important to understand, which factors determine the position of this maximum, and what influence C_l and C_d have over it. For the following analysis only the linear region of the C_l curve is considered. For small incidence angles, the lift curve can be approximated to a first order polynomial, and the drag curve can be approximated to a second order polynomial. Such parameterizations are as stated in Eq. (1).

$$C_D = \mu(\alpha - \alpha_{0d})^2 + C_{Do}$$
$$C_L = m(\alpha - \alpha_{0l}) \tag{1}$$

The lift/drag curve can be expressed as

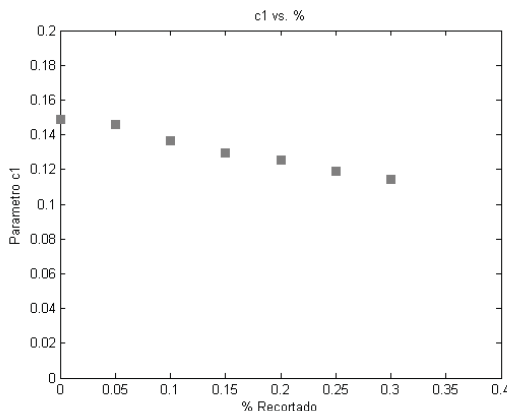$$\frac{C_L}{C_D} = \frac{m(\alpha - \alpha_{0l})}{\mu(\alpha - \alpha_{0d})^2 + C_{Do}} \tag{2}$$

Finding the maximum for Eq. (2) the result is:

$$\frac{\partial}{\partial\alpha}\left(\frac{C_L}{C_D}\right) = \frac{m\left[\mu(\alpha - \alpha_{0d})^2 + C_{Do}\right] - 2m\mu(\alpha - \alpha_{0d})(\alpha - \alpha_{0l})}{\left[\mu(\alpha - \alpha_{0d})^2 + C_{Do}\right]} = 0$$

(3)

$$(\alpha_{L/D\max} - \alpha_{0d})^2 + \frac{C_{Do}}{\mu} = 2(\alpha_{L/D\max} - \alpha_{0l})(\alpha_{L/D\max} - \alpha_{0d})$$

$$\alpha_{L/D\max}{}^2 - 2\alpha_{0l}\alpha_{L/D\max} + 2\alpha_{0l}\alpha_{0d} - \alpha_{0d}{}^2 - \frac{C_{Do}}{\mu} = 0$$

(4)

Equation (4) can be solved to obtain the angle at which the curve of C_l/C_d is at its maximum.

$$\alpha_{L/D\max} = \alpha_{0l} + \sqrt{(\alpha_{0l} - \alpha_{0d})^2 + \frac{C_{Do}}{\mu}} \tag{5}$$

A quick inspection of Eq. (5) allows it to be represented geometrically, as shown in Fig. 8. The angles α_{0l} and α_{0d} represent the angle at which the value of the lift coefficient equals 0, and the angle at which the drag coefficient is a minimum respectively. C_{d_0} is the value of the drag coefficient corresponding to α_{0d}.

Analyzing Fig. 8, it is seen, that probably the most significant variations on $\alpha_{l/d\max}$ can be obtained
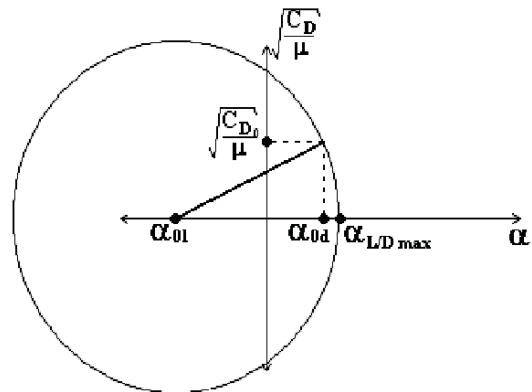

Figure 7. Parameter c_1 for different Λ's for airfoil NACA 4415.

(Drawn with MatLab ©)

Figure 8. Geometrical representation of $\alpha_{l/dmax}$

by displacing the angle α_{0l} to the right or increasing C_{d_0}, which is precisely what happens as the cut-off length increases. Making this angle larger also reduces the value of the maximum C_l/C_d relation, which is also reduced by the fact that C_{d_0} becomes bigger as the cut-off length increases. The latter analysis is developed for the sake of understanding the individual effects of C_l and C_d on $\acute{a}_{l/d_{max}}$.

SOLUTION OF JOUKOWSKI PROFILES

Making use of a conformal transformation of the form $z = \zeta + \dfrac{l^2}{\zeta}$, being z and ζ complex variables, a circle in the ζ space, as represented by $\zeta = re^{i\theta}$ can be transformed into profiles with different characteristics as it is shown ahead [6]. This transformation has the characteristic of mapping a circle or radius l in the $\zeta-$ plane into a straight horizontal line in the z plane. Circles in the ζ plane with radius greater than l will be mapped into ellipses. Thus, applying this transformation to circles whose centres lie on the real axis of the complex plane, these can be mapped into profiles which have an elliptic leading edge and sharp trailing edge. Circles whose centres lie on the imaginary axis of the complex plane ζ will be mapped into cambered lines. Thus combining both transformations, a circle on the $\zeta-$ plane given by $|\zeta - s| = a$ can be transformed into an aerodynamic profile with a cambered chord line with an elliptic leading edge, and a sharp trailing edge. The family of profiles obtained is called the Joukowski profiles (see Fig. 9) [6]. Writing the complex potential w for the flow around a circle of a uniform wind of speed V and incidence angle α, the velocity can be found in the ζ-plane.

$$w = V\zeta e^{i\alpha} + \frac{Va^2 e^{-i\alpha}}{\zeta - s} + 2aiV \sin\beta \log(\zeta - s)$$
$$ae^{i\beta} = e^{i\alpha}(l+s)$$

(6)

Then, the velocity in the z-plane can be found as

$$\frac{dw}{dz} = \frac{dw}{d\zeta} \cdot \frac{d\zeta}{dz} = \frac{dw}{d\zeta} \cdot \frac{\zeta^2}{\zeta^2 - l^2} \qquad (7)$$

$$\frac{dw}{dz} = Ve^{i\alpha}\left(\zeta + l - 2ae^{-i\alpha}\cos\beta\right)\frac{\zeta^2}{(\zeta - s)^2(\zeta - l)}$$

(8)

The velocity is then $u - iv = \dfrac{dw}{dz}$. With the velocity field and knowing the pressure far away from the profile, Bernoulli's equation can be used to find the pressure distribution throughout the profile and in this manner compute the total force acting on the profile due to pressure alone.

The theoretical lift curve is computed after finding the total force per unit length on the profile which is of the form $F = \oint_C p \cdot \vec{dl}\, e^{-i\frac{\pi}{2}}$. The term $e^{-i\frac{\pi}{2}}$ indicates a rotation of 90º in the clockwise direction, so that the pressure acts perpendicular to the surface of the profile.

To simulate the effect of tailoring the trailing edge, the same integral may be computed, but omitting the forces on the percent of the chord to be cut off. These results can be seen in Fig. 11. The fact that this computation may indeed be done as a first approximation to the theoretical solution of the problem, lies in the fact that the pressure distributions vary little when the trailing edge is tailored (see Fig. 10). The flow doesn't "know" about the tailored trailing edge ahead. The only difference in the pressure distributions will be a greater pressure (less suction) on the suction side of the profile due to increased trailing edge dead fluid pressure.

It can be seen from the results how α0l displaces itself to the right as the cut-off length increases. These results are computed considering a potential flow around the airfoil, which is clearly not the case due to the separation that occurs at the trailing edge. The latter analysis does not take into account the fact that the stagnation region behind the profile increases the trailing edge pressure. This has as a consequence a reduction of fluid speed on the suction side of the

profile, and thus greater static pressure (Bernoulli's equation). Having greater static pressure on the suction side of the profile causes a decrease in the lifting force, and thus lower values of Cl as seen in Fig. 11.

Both effects combined (greater pressure at the trailing edge and α0l displacement) lead to a lift coefficient variation as seen in Fig. 3.
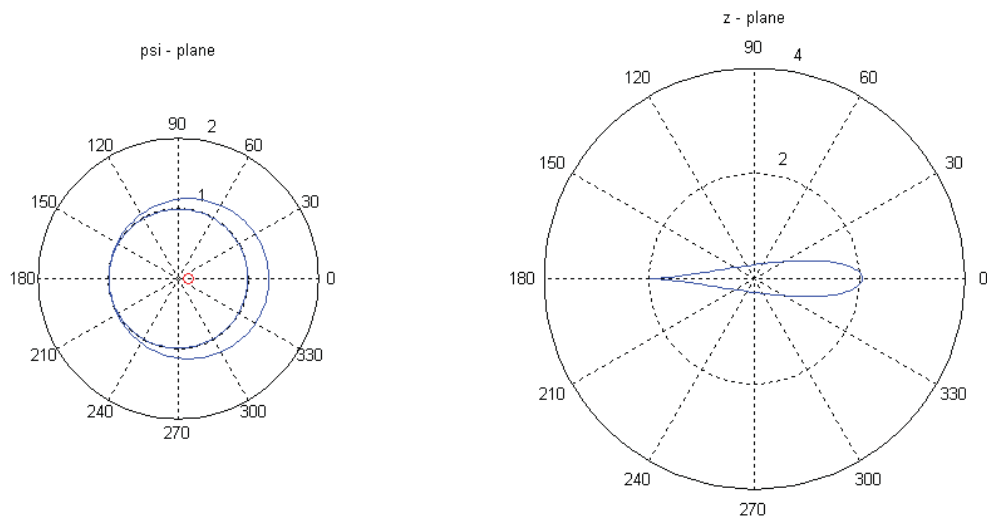

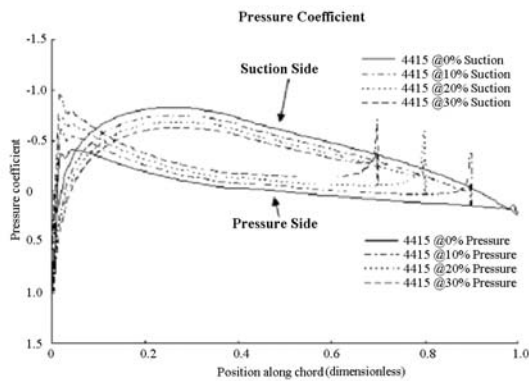Figure 9. General Joukowski profile. (Drawn with MatLab ©)

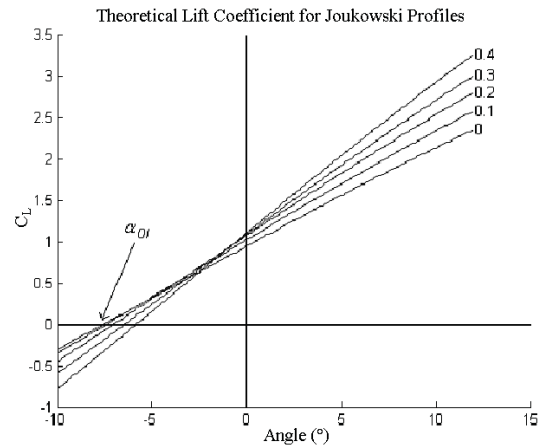Figure 10. Pressure coefficient for modified profiles

Figure 11. Effects on Cl due to tailoring the trailing edge.

(Drawn with MatLab ©)

CONCLUSIONS

The following conclusions may be drawn from the parameterization of the NACA profiles:

• The behaviour of profiles subjected to trailing edge modifications is similar within profiles of the same relative thickness.

• Thinner profiles have higher C_l/C_d ratios.

• Thicker profiles have higher angles corresponding to the maximum C_l/C_d ratios.

• For thicker profiles, steeper slopes of parameter a_1 are found, meaning that these are more sensible to trailing edge modifications.

• The greater the camber of the profile, the greater the displacement of parameter b_1 (angle at which the greatest C_l/C_d ratio occurs).

• The greater the camber and the thickness, the wider the distribution of the C_l/C_d values, which means a slower increase in drag values.

Allowing modifications at the trailing edge of NACA profiles influences the behaviour of both lift and drag coefficients. The two most important characteristics are the increase of αl/dmax and the changes of the stall behaviour of the airfoil.
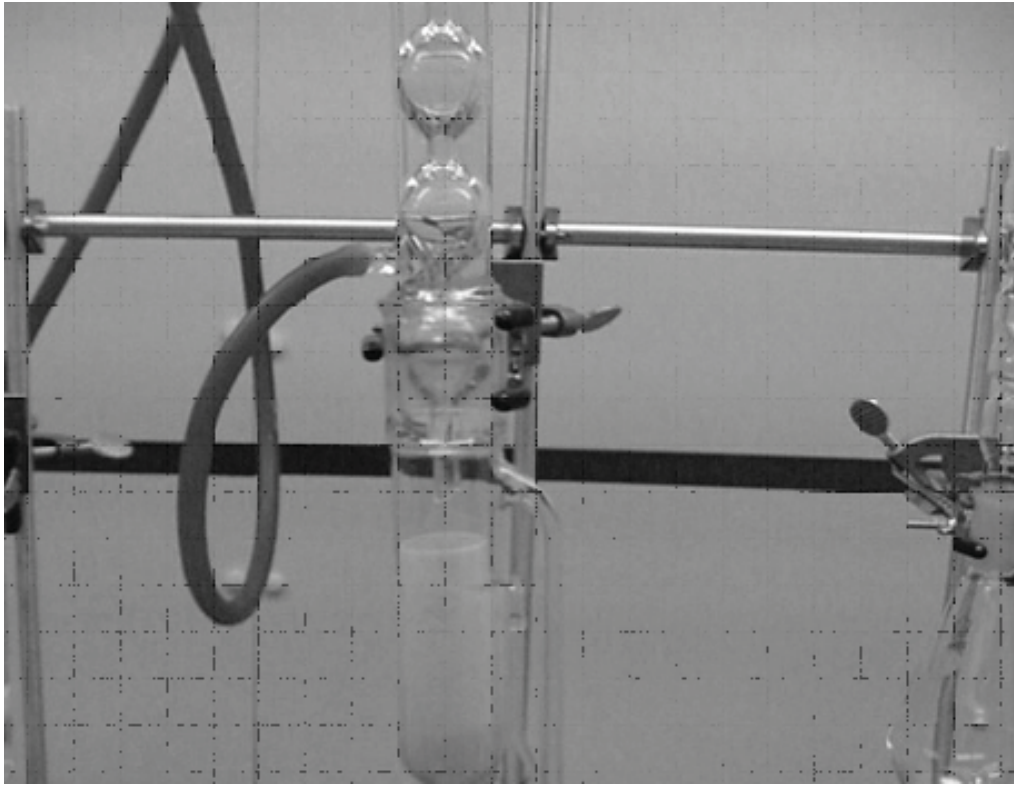
The implications on manufacture of the proposed modifications can be summarized as a simplified construction of the profile, because the trailing edge must not be manufactured to a knife-sharp edge, but imperfections may be allowed.

Although the consequences regarding the manufacture of airfoils are very important, further work is required to determine the benefits that can be achieved by having higher values of b1 and flatter Cl/Cd curves. For example, with higher values of b1, the positioning of the profiles in a wind turbine can be made in such a way that higher lift coefficients can be achieved.
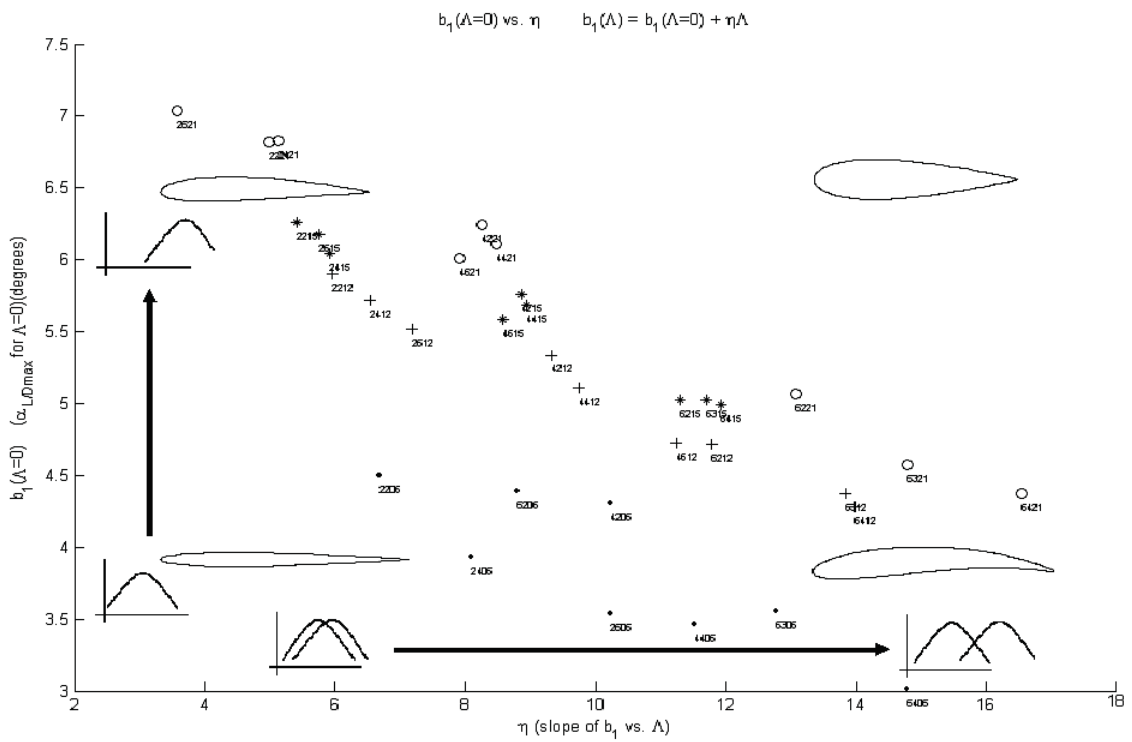
Experimental validation of these computational findings is expected to be carried out once the wind tunnel facility of the Universidad de Los Andes becomes operational in 2007.

REFERENCES

[1] **D.R. Chapman, R.H.Kester.**
"Effect of Trailing Edge Thickness at Supersonic Velocities". Ames Aeronautical Laboratory. NACA RM A52D17. Washington. 1952.

[2] **J.L Summers, W.A. Page.**
"Lift And Moment Characteristics at Subsonic Mach Numbers of Four 10 Percent Thick Airfoil Sections of Varying Trailing Edge Thickness". Ames Aeronautical Laboratory. NACA RM A50J09. Washington, 1950.

[3] **J. Herrig et. al.**
"Effect of Section Thickness and Trailing Edge Radius on the Performance of NACA 65- Series Compressor Blades in Cascade at Low Speeds". NASA RM L51J16. 1951.

[4] **J.J. Moses, G.K. Serovy.**
"Some Effects of Blade Trailing Edge Thickness on performance of a Single-Stage Axial Flow Compressor". Lewis Flight Propulsion Laboratory. NACA RM E51E28. Washington, 1951.

[5] **E.N. Jacobs, K.E. Ward, R.M Pinkerton.**
"The Characteristics of 78 Related Airfoil Sections from Tests in the Variable Density Wind Tunnel", NACA report 460, N.A.C.A, 1932.

[6] **L. M. Milne Thomson.**
Theoretical Aerodynamics. New York: Dover Publications, Inc., 1958.

[7] **I. H Abbott, A. Doenhoff.**
Theory of Wing Sections. New York: Dover Publications, Inc., 1959.

[8] **E.H. Lysen.**
"Introduction to Wind Energy". CWD – Consultancy Services Wind Energy Developing Countries. Amersfoort, 1983,

[9] **T. Burton et al.**
Wind Energy: Handbook. New York: John Wiley and Sons, 2001.

APPENDIX A

APPENDIX B